THE PG1159 VARIABLES

Arthur N. Cox
University of California
Theoretical Division
Los Alamos National Laboratory
Los Alamos, New Mexico 87545

The PG1159 variables, named after the variable of that number in the Palomar-Green blue star catalogue, have high luminoisites, high surface temperatures, and high gravities. Their masses, however, must be the normal low value of 0.6 solar mass because they are the direct antecedents of the classical DB white dwarfs. In every case, they seem to have no hydrogen at all in their atmospheres, but significant helium, carbon, and oxygen is present (Sion, Liebert, and Starrfield 1985). Table 1 gives a list of these stars of which most, but not all, show light variations indicative of nonradial low degree, but probably high order, g modes.

The discovery of the prototype variable of this class was by McGraw, Starrfield, Angel, and Carlton (1979). Early work on the theoretical interpretation has been given by Starrfield, Cox, Hodson, and Pesnell (1983), and Starrfield, Cox, Kidman, and Pesnell (1984, 1985). I include here the variable star Kl-16 (Grauer and Bond 1984), the central star in an old planetary nebula, even though it is on the constant luminosity branch preceding the white dwarf constant radius cooling track. Recent observations for periods of two of these PG1159 stars are given by Bond, Grauer, Green, and Liebert (1984).

Work done at Los Alamos with Starrfield and Kidman, using the new Lagrangian-based linear nonradial pulsation eigensolution program of Pesnell, has assumed that the surface temperatures are all above 80,000 K, the luminosities range between 100 and 10,000 suns, and that the helium abundance is so low that it can be ignored in the pulsation calculations. This latter assumption is made because the presence of even 25% of the surface layer mass as helium dilutes the normal kappa and gamma effects of the carbon and oxygen to such an extent that the stars are not pulsationally unstable. More study is urgently needed to observationally estimate the helium abundance, especially to see if the poisoning effect of helium revealed in the nonadiabatic calculations leads to an inconsistency between observed and theoretical (pulsation based) abundances.

The concept is that these stars have lost even more surface layers than the usual pre-white dwarfs, which eventually float their hydrogen to the surface to become the predominant DA white dwarfs. We here assume that the small residual helium will float to the surface in the time needed to cool down to about 80,000 K, and these PG1159 variables will all become just DB stars. The presence of oxygen, as actually observed in the spectrum, is crucial to make these stars pulsate, but again it is not yet clear how much is required. These stars have been skinned off so much that they show layers that were so deep in the red giant stages of evolution that considerable oxygen was produced in the helium shell flashes. Thus for this report, the composition assumed is half carbon and half oxygen by mass; the observed helium is considered to be negligible.

While it is conceivable that these stars can pulsate due to the modulation of the nuclear energy generation by helium burning (ε effect), work by Kawaler in Texas shows that only the lower order, shorter period modes actually are unstable to pulsations. This undoubtedly is because the higher order modes have so many nodes in the deep helium burning layers that there is little amplitude at that position. However, the presence of deep helium is not likely if oxygen is already easily seen at the surface. Since these are very old stars, any deep helium should have already been burned away at depths where modulation of the source would be strong enough to drive pulsations.

We here discuss in detail a 0.6 solar mass model that has a temperature ranging from 100,000 K for its surface effective temperature to a maximum of almost 200 million K, and then a decrease to about 85 million K at the center. This temperature inversion is caused by strong neutrino losses at the high central densities. These internal densities range from 10^{-6} to 10^{+6} g/cm^3 from the surface to the center. For luminosities considerably lower than the 1.075×10^{35} erg/sec for this model, the central temperature inversion disappears and the central density grows larger. For the PG1159 class of stars however, there is always this inversion.

Figure 1 gives the key quantity for the kappa effect, the logarithmic derivative of the opacity with respect to the temperature. The bump near zone 500 is due to the decrease in the negative slope of opacity with temperature caused by the ionization of carbon and oxygen near temperatures of 10^6 K. This bump causes the opacity to actually increase upon compression in a pulsation. Higher density always produces higher opacity in stellar envelope material, but usually the simultaneous higher temperature gives a larger opacity decrease to let radiation flow more easily during compression. With a large enough bump, the resulting opacity increase can block the radiation flow periodically to give pulsation driving.

This kappa effect is often enhanced by the gamma effect, especially if the bump pictured in Figure 1 is due to ionization of an abundant ion. In that case, the rapid increase of ionization with temperature results in a significantly lower gamma and a much larger compressibility. Therefore, the opacity is even more increased during compression because the density can grow even larger for the same increase in temperature. Figure 2 plots the Γ_3-1 versus zone number in the model, and the very low gamma in the driving region is seen. The large variations for the zones deeper than zone 350 have little effect on the pulsation solution. One can see that there is a table change at zone 300 to one with finer spacing of the entries, and at zone 200 there is a change to the Iben analytic fit for the material properties. If there is not too much inert material in the driving layers, the kappa and gamma effects can give strong radiation blocking and enough pulsation driving to overcome any deeper radiation leaking which damps the oscillation. Considerable helium, fully ionized at the million kelvin temperature, would void the gamma decrease as well as the opacity bump to poison the potential driving effect.

Note that the kappa and gamma effects need an opacity bump and a significant decrease in the gamma. It seems that the last ionization of a dominant abundance element is the only one that gives this behavior because the ionization energy is much larger than for ionization of the less tightly bound electrons. This isolates the kappa increase and the gamma decrease, which then can be large enough to give radiation blocking.

Figures 3 and 4 give the radial and horizontal eigenvectors of the pulsation for the g_{15} $\ell=1$ mode. All the many nodes in the layers deeper than zone 400, as well as the very nearly adiabatic structure at these depths, give small pulsation amplitudes there. Note that the horizontal motions are about 250 times the radial ones at the surface. The high gravity of the model makes radial motions difficult.

The last figure for this model gives the driving per zone for this mode for all the 600 layers of the model. The kappa and gamma effects driving is largely cancelled by the radiative damping down to zone 400 (almost 10 million kelvin), but the small net positive work each cycle allows the amplitudes to e-fold each 1000 cycles. The damping is interrupted near zone 470 because of a decrease in the density variation caused by the combined effect of the radial and horizontal motions. At a period of 495 seconds, this is a typical period for the PG1159 variables.

Tables 2 and 3 give, respectively, $\ell=1$ periods, growth rates and kinetic energies for two models. The data in Table 2 are for a typical variable like PG1159-035 at 100,000 K. Modes with periods shorter than 127 seconds (g_3) are stable as are modes with periods

longer than 562 seconds (g_{17}). One can see that the kinetic energy
for the longest periods (with smallest deep motions) is the smallest
of all the modes. That means that it takes less energy to make the
mode observable, and these 400-600 second periods should be the
easiest to occur. Fortunately, that is what is actually observed.

The data in Table 3 are for a model at 130,000 K on the high luminos-
ity track, typical of the planetary nebula central star K1-16. The g
modes 37 to 57 are listed again for $\ell=1$. Modes 42, 44, and 46 seem
to have the smallest kinetic energies with periods from 2554 to 3098
seconds. In this case, these most unstable periods are almost twice
the observed ones, but that problem can be cured by reducing the
radius of the model to 0.70 that used here making the effective
surface temperature 155,000 K. The many uncertainties such as effec-
tive temperature and the exact internal structure have prevented any
actual mode identification in any pre-white dwarf or white dwarf
variable star.

Recent observations have shown that the observed mode for PG1159-035
at 516 seconds is decreasing its period at an e-folding rate of
2.34×10^{-14} s^{-1}. Early studies by Kawaler, Hansen, and Winget
(1985) predicted period increases due to the deconcentrating of the
structure. Any slight shrinking that might decrease the period was
overwhelmed by the change in the pulsation constant. The latest
result is that the observed period decrease is due to a further
effect, the spinup of the stellar surface during evolution. If the
mode is prograde, the time between the l=3 m=-3 sectorial mode merid-
ian crossings grows shorter as the star rotates faster, presenting an
apparent period decrease to an observer. This work by Kawaler,
Winget and Hansen (preprint) then predicts a rotation velocity of
35-50 km/sec, not unreasonable for a white dwarf.

The expectation is that these stars will eventually float their
helium to the surface to cover all the carbon and oxygen. They then
will be DB stars. However, unless the helium is in a shell thick
enough to give the convection blocking predicted by Cox, Starrfield,
Kidman, and Pesnell (preprint), these particular DB stars will not
pulsate. Calculations show that convection is not strong enough in
the CO mixtures to give the pulsation driving seen in the pure H (DA)
and He (normal DB) stars.

The last figures illustrate this convection blocking in a DA case at
13,000 K. Figure 6 gives the work per zone plot showing that the
peak driving is in zone 515. Inspection of the model shows that the
temperature there is about 80,000 K, much too hot even at these high
densities for hydrogen ionization to be still occurring. Actually
the small bump at zone 537 at 27,000 K is the kappa and gamma effect
work from the hydrogen ionization. Figure 7 gives the logarithmic
derivative of the opacity with temperature, which shows no opacity
bump, but at least not such a negative slope at zone 537. The deeper

driving is due to the blocking effect of luminosity because of the way we treat convection as unchanging throughout the pulsation cycle. Some adaptation of the convection luminosity happens in the real case, and the convection blocking will be less than we have here. Just how much less is a problem for the yet-to-be developed time dependent convection theory. Figure 8 shows the static model luminosity fraction due to radiation; the strong blocking of the luminosity by convection makes this model pulsationally unstable.

TABLE 1

PG1159 Stars

Star	V	Periods
PG0122+200	16.1	need more data
PG1151-029	16.4	?
PG1159-035	14.84	460,540 sec
PG1424+535	16.2	No
PG1520+525	15.52	No
PG1707+427	16.4	386,413 sec
PG2131+066	16.63	450 sec
K1-16	15	1520,1730 sec
VV 47		Yes

TABLE 2
Summary Table for $\ell=1$
0.6 M_θ 100,000 K 1.075 × 10^{35} ergs/s

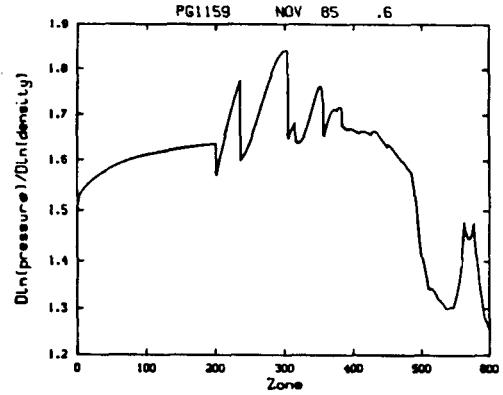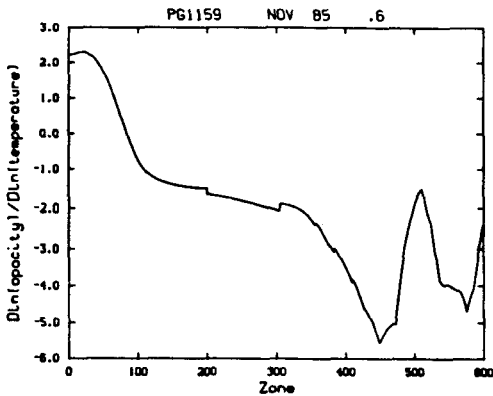| Number of g-Type Nodes	Non-Adiabatic Period (seconds)	Predicted Growth Rate (KE/cycle)	Total Kinetic Energy (ergs)
17	562	1.9e-04	2.3e+44
16	530	9.1e-04	1.9e+44
15	495	1.0e-03	2.3e+44
14	467	6.6e-04	4.4e+44
13	430	6.5e-04	3.9e+44
12	405	2.5e-04	1.0e+45
11	367	1.7e-04	9.9e+44
10	342	6.5e-05	2.5e+45
9	307	2.3e-05	3.6e+45
8	281	6.8e-06	1.2e+46
7	246	1.9e-06	1.2e-46
6	220	4.2e-07	8.3e+46
5	187	5.8e-08	6.4e+46
4	160	1.2e-08	1.5e+48
3	127	4.5e-10	2.5e+47

Figure 1. The logarithmic dervative of the opacity with respect to
the temperature for the PG1159-035 model.

Figure 2. The Γ_3-1 versus zone number showing the deep dip due to
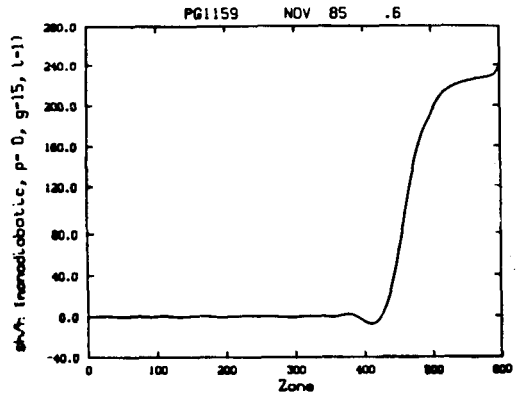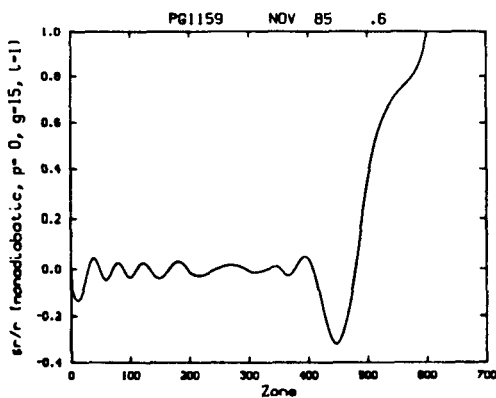carbon and oxygen ionization.

Figure 3. The radial eigenvector showing the relative motion for the
ℓ=1, g_{15} nonradial mode for the PG1159 model.

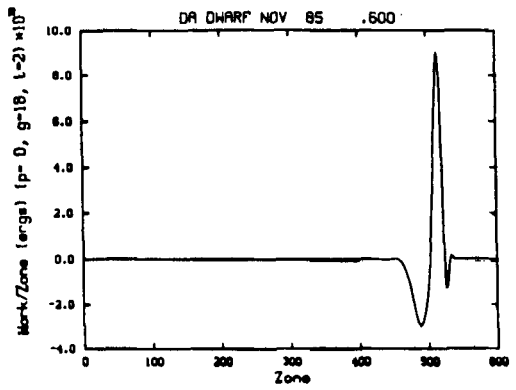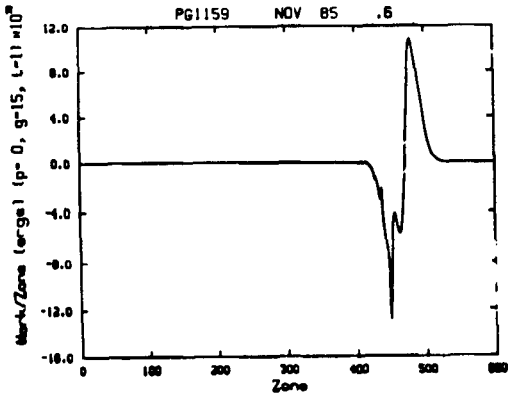Figure 4. The relative horizontal motion in the PG1159-035 model.

Figure 5. The work per zone each pulsation cycle to drive or damp the oscillation plotted versus Lagrangian zone number.

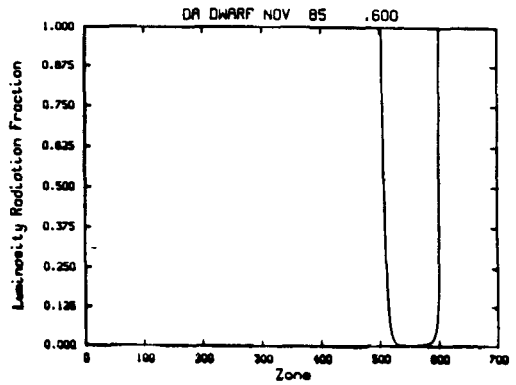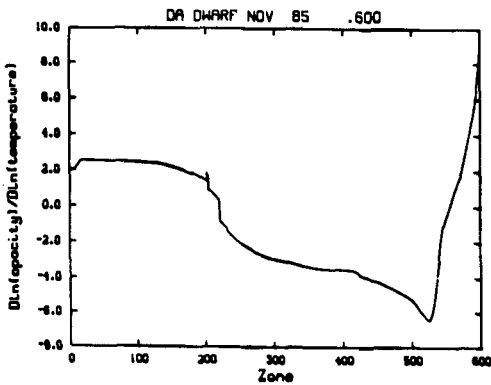**Figure 6.** The work per cycle to create pulsations versus zone number for the 13,000 K white dwarf model.

Figure 7. The logarithmic derivative of the opacity with respect to temperature versus zone number for a 13,000 K white dwarf model.

Figure 8. The fraction of the luminosity due to radiation flow is plotted versus Lagrangian zone number for the white dwarf model.

TABLE 3
Summary Table for $\ell=1$
0.6 $M_\odot$ 130,000 K 1.96 × 10^{37} ergs/s
Summary Table for $\ell=1$

Number of g-Type Nodes	Non-Adiabatic Period (seconds)	Predicted Growth Rate (KE/cycle)	Total Kinetic Energy (ergs)
57	5313	9.4E-03	1.2E+45
56	4992	1.3E-02	1.5E+45
55	4816	2.6E-03	1.2E+46
54	4629	1.5E-02	1.5E+45
53	4316	1.4E-02	1.4E+45
52	4149	2.7E-03	1.5E+46
51	3988	1.2E-02	1.3E+45
50	3711	9.1E-03	1.7E+45
49	3620	3.6E-03	4.5E+45
48	3392	8.8E-03	1.0E+45
47	3243	1.3E-03	6.9E+45
46	3098	6.8E-03	8.1E+44
45	2926	1.0E-03	5.0E+45
44	2818	4.8E-03	6.9E+44
43	2656	6.4E-04	4.7E+45
42	2554	2.4E-03	7.5E+44
41	2421	2.8E-04	5.6E+45
40	2311	8.6E-04	1.1E+45
39	2213	9.4E-05	8.2E+45
38	2077	1.4E-04	3.8E+45
37	2016	6.5E-05	5.4E+45

References
Bond, H. E., Grauer, A. D., Green, R. F., and Liebert, J. W. 1984, Ap. J. 279, 751.
Grauer, A. D. and Bond, H. E. 1984, Ap. J. 277, 211.
Kawaler, S. D., Hansen, C. J., and Winget, D. E. 1985, Ap. J. 295, 547.
McGraw, J. T., Starrfield, S. G., Angel, J. R. P., and Carlton, N. P. 1979, Smithsonian Ap. Obs. Spec. Report, No. 385, p 125.
Sion, E.M., Liebert´,J. W., and Starrfield, S. G. 1985, Ap. J. 292, 477.
Starrfield, S. G., Cox, A. N., Hodson, S. W., and Pesnell, W. D. 1983, Ap. J. 268, L27
Starrfield, S. G., Cox, A. N., Kidman, R. B., and Pesnell, W. D. 1984, Ap. J 281, 800.
Starrfield, S. G., Cox, A. N., Kidman, R. B., and Pesnell, W. D. 1985, Ap. J. 293, L23.